

Fig. 9-1. Double rainbow in the rain shaft beneath the thunderstorm of 23 Jul 2018 east of Cheyenne, WY. Jan Curtis.



Fig. 9-2. Double rainbow crossed by anticrepuscular rays at Cheyenne, WY 08 Jun 2024. Jan Curtis.

Wonders of the Atmosphere Chapter 9: Rainbows, Fog Bows, and Rays

Started 24 Dec 2024

9.1 Observations and Properties of Rainbows

Tranquility reigns and the blue sky gleams because the late afternoon thunderstorm of 23 July 2023 shown in Fig. 9-1 has moved off to the east of Cheyenne, WY. The Sun, low in the western sky, illuminates the retreating cumulonimbus cloud. In the darker, but sunlit rain shaft beneath the cloud a bright segment of a rainbow appears, red on the outside of the arc and almost spectral, though deficient in blue. That is the primary rainbow. A faint secondary bow with colors in the opposite order, appears outside (to the right of) the primary bow.

How can it now be so peaceful when just minutes before it was so dark, so terrorizing, and so destructive beneath that same cloud? It is fitting that such an observation was memorialized and given great significance in the Book of Genesis of the Bible.

I have set My bow in the cloud, and it shall be for a token of a covenant between Me and the earth...and you and every living creature of all flesh; and the waters shall no more become a flood to destroy all flesh. *King James Bible*, *Genesis*, Ch. 9.

Forgetting for the moment that rainbows appear in the rain shafts below the clouds it is true that outside the tropics rainbows are usually seen after the storm and all its fury have passed because, 1: most thunderstorms occur in the afternoon, when the Sun is in the west, 2: rainbows appear opposite the Sun and, 3: the prevailing wind aloft outside the tropics drives thunderstorms from west to east. In the tropics, rainbows have been taken a warning of impending doom because the prevailing winds aloft blow in the opposite direction – from east to west, so that rainbows are often seen just before the thunderstorm blots the sky and wreaks its havoc.

Rainbows are produced when sunlight strikes raindrops. Each drop acts like a prism and a mirror. Sunbeams are refracted upon entering a drop. They are then reflected inside the drop either once for the primary bow or twice for the secondary bow. After the reflections, the beams are refracted a second time on exiting the drops.



Fig. 9-3. A double rainbow from spray drops from a garden hose. SDG.

The relative intensity of scattered light striking a raindrop as a function of scattering or deflection angle was shown in the red curve in Fig. 1-16. It shows a deep, flat valley walled in by abrupt increases on each side – by factors of more than 100 to the peak of the primary rainbow at 138° (42° from your shadow at the antisolar point) and, more than 25 to the peak of the secondary bow at 129°. The primary bow is about 2° wide with red on the outside (at 42.5°) and violet on the inside. The secondary bow is about 3° wide with colors in the opposite order. *Anticrepuscular* rays sometimes cross the bows, always at 90° as they point to the antisolar point (Fig. 9-2).



Fig. 9-4. Drops that produce the rainbow reaching PopEYE. SDG.

In spray from a hose, you can how see myriad individual drops add up to produce the bow (Fig. 9-3). The drops, which were shot out of a hose to the left of the image, appear as streaks because they moved several cm during the camera's finite exposure time. Each drop-streak produces its own minibow but appears to have the color appropriate to its location in the bow, or if the

drop-streak traversed several color bands in the bow it displays those colors. Fig. 9-4 shows that each drop produces an entire spectrum but only one tiny beam of light with just one color reaches PopEYE and all other colored beams from that drop miss PopEYE.

The requirement that drops be sunlit to produce rainbows is why rainbows tend to be associated with thunderstorms, which are often surrounded by clear skies that allow sunlight to strike the rain shaft below the cloud. Nimbostratus clouds, which tend to cover the sky, only produce rainbows in rare breaks in the overcast most likely to occur in the cold, showery sector of departing extratropical cyclones.

The most vivid rainbows occur when the background is dark. In Fig. 9-3 the shaded inside of the garage provided a very dark background while the sunlit garbage pails were so bright they swamped the bow. Similarly, fountain rainbows cannot be seen in the opaque white central column, but only off to the sides in the translucent spray.

The rainbow's beauty is reduced by incoherent background light of the rainshaft, which results from multiple scattering of sunlight off many drops. When the optical thickness of the sunlit rain shaft is small, relatively little light is scattered more than once so that the coherent light that has been scattered off a single raindrop dominates and the rainbow stands out from a dark background. The greatest





Fig. 9-5. Two views, minutes apart of the double rainbow of 21 Jun 2018, east of Cheyenne, WY. Rainbows stand out best against a dark background. Jan Curtis.

contrast between the brightness of the rainbow and the brightness of the rain shaft occurs at optical thickness, $\tau \approx 1$. As τ continues to increase the fraction of light that is is scattered more than once increases more rapidly than the single scattered light that produces the rainbow, so contrast decreases and the rainbow is swamped.

The two images of the double rainbow in Fig. 9-5 demonstrate the crucial role played by lighting *contrast* between the bow and the

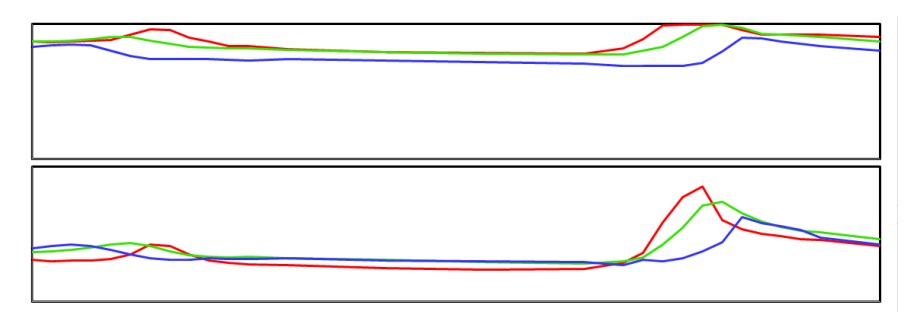


Fig. 9-6. RGB colorimetric analysis of the rainbows of Fig. 9-5. SDG. background in creating a feeling of awe. The bottom image occurred only minutes after the top image. Both are taken from the video,

https://www.flickr.com/photos/cloud_spirit/29073519338/in/album-72177720311456882/lightbox/

In the top image, a much greater optical thickness of the rain shaft was sunlit (while the foreground was shaded) than in the bottom image. As a result, the background skylight was so great in the top image that the rainbows appear washed out with poor color purity. In the bottom image, though the foreground was sunlit, much of the rain shaft and the background sky were shaded and dark. The resulting bow, just about the most dramatic that Jan ever saw, had much greater contrast with the dark background and greater color purity



Fig. 9-7. Double rainbow with sunlit rain streaks on 20 Jun 2017 east of Cheyenne, WY. Jan Curtis.



Fig. 9-8. Primary rainbow just before sunset 26 Apr 2020, Cheyenne, WY. Jan Curtis.

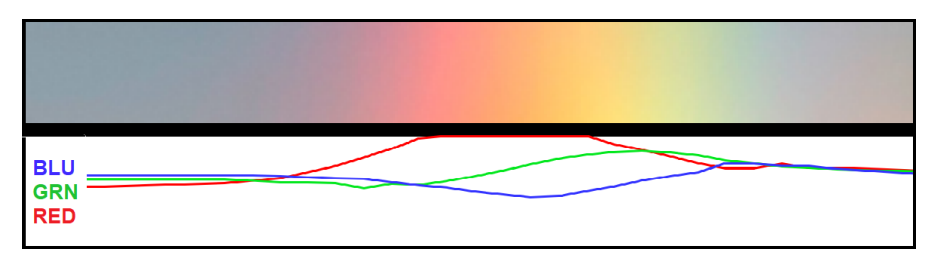


Fig. 9-9. RGB colorimetric values across the sunset rainbow of Fig. 9-4. SDG.

even though its absolute luminosity was 30% lower than the bow in the top image! This is confirmed in Fig. 9-6, the colorimetric analysis of Red, Green, and Blue (RGB) values of the bows. The increase of red is both absolutely and fractionally much larger for the bow with the dark background, and it also has a distinct green band absent from the bow with the bright background. (Photos provide reasonably accurate spectra if they are not under- or overexposed.)



Fig. 9-10. Rainbow just after sunrise, 19 Nov 2016, San Mateo, CA. SDG.

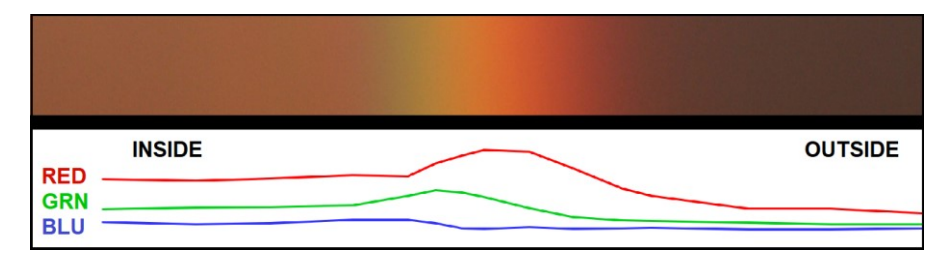


Fig. 9-11. RGB colorimetric values across the dawn rainbow of Fig. 9-5. SDG.

The complete arc of a double rainbow can be a noble sight, spanning up to almost ½ of the way around the horizon as on 20 Jun 2017 east of Cheyenne, WY (Fig. 9-7). The bows were so wide (a maximum of 102°) that seven panels were stitched to produce it with its curved horizon. The photo is reminiscent of Frederic Church's painting, *Rainy Season in the Tropics* (see Fig. 15-6) and the scene's width may be one reason Church cut the distance between the bows in his painting to half of what Nature demands.

In Fig. 9-7 sunlit rain streaks brighten the primary bow and the sky below it in dramatic fashion, though where they are brightest they almost swamp the bow. The contrast between the bow and the dark, clouded background on the right is much greater, than between the bow and the clear, pale blue sky on the left horizon.

As vivid as the colors of the rainbow may seem, they always fall far short of the color purity of a spectrum produced when a slit of sunlight at the zenith passes through a prism. Three main factors limit the rainbow's color purity, 1: A raindrop lacks the eyeball's narrow circular pupil and lens, which focuses a narrow beam of light on the retina in the back of the eye. As a result, because light strikes the entire raindrop it emerges in a diffuse manner with limited focusing 2: Rayleigh and Mie scattering by air molecules remove most violet and blue sunlight before it reaches raindrops, especially when the Sun is near the horizon where the optical path through the atmosphere is large, 3: Skylight and other background light 'drown' the bows and reduce the purity of their colors (as in Fig. 9-5). As a result, rainbow photos with high color purity are always doctored!

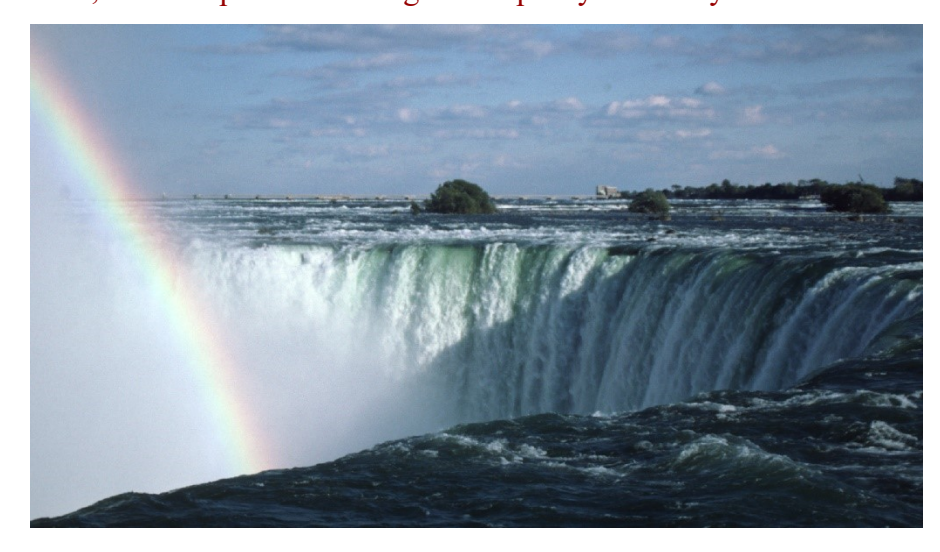


Fig. 9-12. Afternoon spray bow at Niagara Falls. SDG.

Despite the surprisingly large color range and beauty of the sunset rainbow of Fig. 9-8, it suffered from these limitations. Fig 9-9, the

RGB (Red, Green, Blue) colorimetric analysis of the bow shows that even at the red peak, the color purity of the bow is modest at best and blue never dominates in the bow. Outside the bow blue skylight prevails. The only reason that this sunset bow had such a large range of colors is that Cheyenne, WY is 1850 m above sea level, where pressure is 20% lower than at sea level, so that some of the shorter waves reached the rain shaft.

At sea level, red dominates sunrise and sunset bows to a high degree because almost all the short waves have been scattered before reaching the rain shaft. The bright sunrise bow on 19 Nov 2016 at San Mateo, CA (Fig. 9-10) is a case in point. Even though we FEEL sure that the bow has a yellow and green band, red is the dominant color for the entire bow as shown in the colorimetric analysis of the RGB values across a rectangular section enocmpassing the bow just above the level of the apartment (Fig. 9-11). Green has its maximum



Fig. 9-13. Double rainbow in Oahu from a nearby sun shower with mountains in the background. ©Rudy Fernberg.

value where we 'see' green, but even at that point, red is dominant. The optical illusion derives from the nature of human color perception, where we judge the color of some region in the vision

field by the surrounding colors. Covering all but the bow's 'green' region shows that its color is, in fact, a tone close to buff or camel.

When the Sun is not near the horizon the primary rainbow is often quite colorful. Even so, its color sequence, with red on the outside, is often ignored or blatantly reversed, as in the 1940 film, *Fantasia*. Perhaps the artists worried that they could not violate Nature's Copyright. Perhaps they were representing the secondary bow, whose color sequence is opposite that of the primary.



Fig. 9-14. A glass bead bow in the street forms a circle around the camera. Glass bead bows are close to half the size of rainbows. SDG.

Even less often do people notice that the sky is brighter inside than outside the primary bow, For example, the sky in Fig. 9-10 is much darker outside (to the right in this case) of the rainbow, and this is confirmed quantitatively in Fig. 9-11. A more subtle observation occurs when the primary and secondary rainbows are both present, as in Fig. 9-1, both frames of Fig. 9-4, and Fig. 9-5, etc.). There, the sky

is darkest between the two bows in a region called Alexander's Dark Band (which is pronounced in the 'valley' of Fig. 1-16), after Alexander of Aphrodisias, who described it around 200 CE.



Fig. 9-15. A 360° double rainbow in a rain shower above Cottesloe Beach in western Australia in 2013. Colin Leonhardt colin@birdseyeview.com.au

In most sightings and photographs, rainbows are cut off by the horizon. That is only because in most settings there are too few raindrops between the observer and the ground to produce a visible bow. All it takes is a view into the chasm of a waterfall such as Niagara (Fig. 9-12) or a nearby sunshower in Oahu, Hawaii (Fig. 9-13) with dark hills in the background to dispel that notion.

Without any obstacles it is possible to see the full circle rainbow. The almost full circle bow of Fig. 9-14 was produced not by rain but by the tiny spherical glass beads incorporated in traffic paint to improve its reflection. Because the index of refraction of glass, $n_{\rm GLASS} \approx 1.51$, the glass bead bow forms 21° from the antisolar point instead of 42° produced by raindrops. The lines were freshly spray painted, so, some glass spheres bounced outside the lines and spread around the

pavement. Glass bead street bows last until the spheres are crushed, blown away by the wind, or ironically, washed away by rain.

Full circle rainbows can only be seen from elevated vantage points.such as airplanes, mountain peaks, cliffs, or near spray from a garden hose, because it is in these situations where the veil of sunlit drops can surround or envelop the observer. Fig. 9-15, taken at Colin Leonhardt's expense during a flight over Cottesloe Beach, shows the full 360° primary bow, most of the secondary bow, and Alexander's Dark Band.

9.2 The Geometric Optics Rainbow

Most of the features of the primary and secondary rainbows can be

explained or at least modeled and simulated accurately with a few simple laws. The main simplification is to use geometric optics, which treats light as beams that obey the laws of reflection and refraction. These laws are then applied to circular cross sections that pass through the centers of spheres, a close approximaton for all but very large raindrops (recall Fig. 4-4 and Fig. 4-5).

The rays that produce the primary rainbow follow the path shown in both panels of Fig. 9-16.. They strike the drop at incidence angle, i, are refracted and pass into the drop at refraction angle, r. The rays then proceed to the back of the drop where they are reflected inside the drop at angle r. Finally, they exit the drop at angle, i, after being refracted for the second time.

Sunbeams strike all over each raindrop so i can be any angle from 0° (dead center) to $\pm 90^{\circ}$ (top/bottom fringe). In the left panel we set

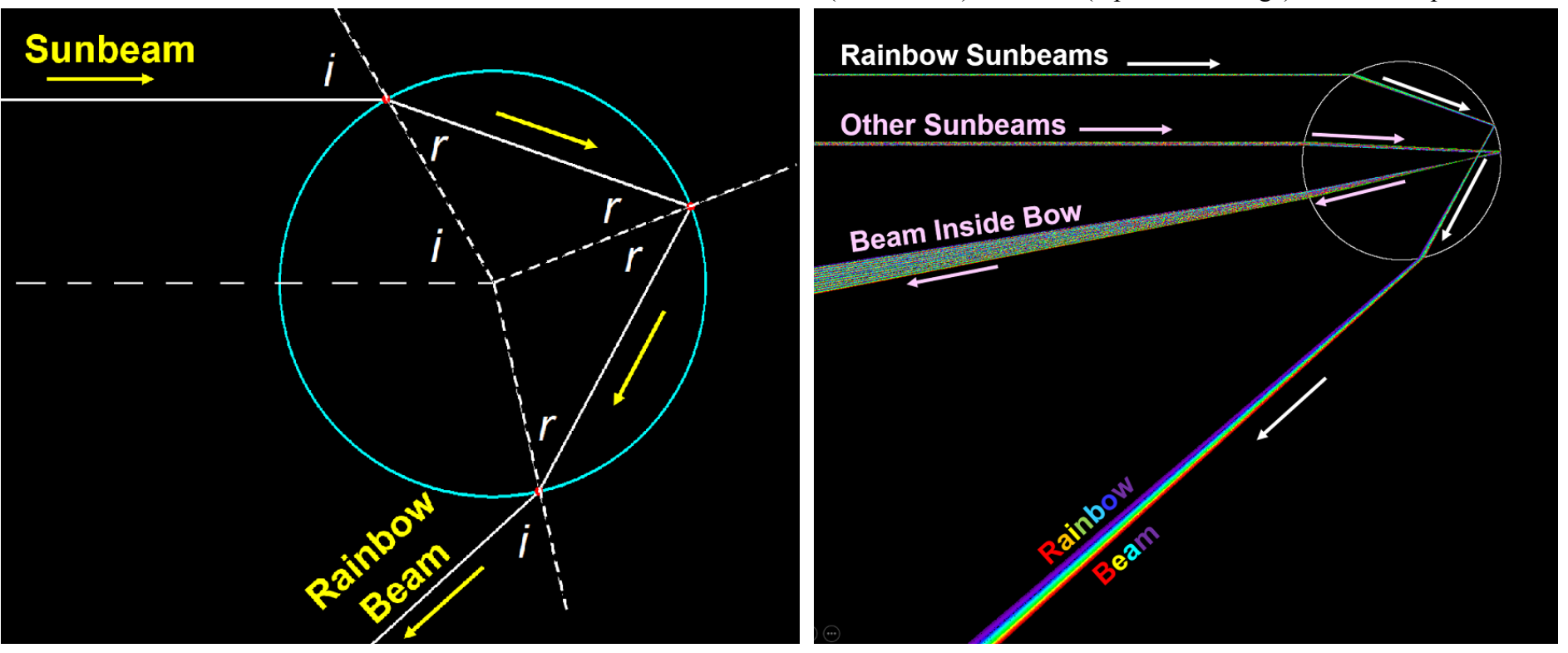


Fig. 9-16. Left: Geometric optics of the rainbow beam with incidence angle $i \approx 60^{\circ}$ and refraction angle $r \approx 40.2^{\circ}$. Right: Narrow bundle of rainbow beams with near spectral colors vs. broader bundle of white beams at all other incidence angles. SDG.

angle, $i = 60^{\circ}$, which is very close to the beams that produce the primary rainbow. Then, angle $r \approx 40.2^{\circ}$.

When light strikes a raindrop and undergoes one reflection and two refractions it will return at angles between 0° and 42° from your shadow depending on where they strike the drop. For example, the light beam that hits the center of the raindrop will bounce straight back at a 0° angle from your shadow.

A problem is why only the beams that emerge at 42° contribute to the primary rainbow and exhibit colors. The right panel of Fig. 9-16 illustrates this. Two bundles of several thousand beams each, were aimed at the raindrop. The top bundle struck the drop at a small range of angles around $i = 60^{\circ}$. It produced the focused primary bow with near spectral color segregation. The bottom bundle struck the drop at a small range of angles around $i = 10^{\circ}$. It emerged as a broader, less focused, near-white mixture (which appears inside the primary bow).

In 1637, Rene Descartes solved one part of that problem in an appendix to *A Discourse on Method*. He aimed a series of parallel sunbeams at a spherical globe filled with water and then used the laws of refraction and reflection to trace their paths through the drop.

The principal difficulty still remained, which was to determine why, since there are many other rays which can reach the eye after two refractions and one or two reflections when the globe [raindrop] is in some other position, it is only those of which I have spoken which exhibit the colors.

I then took my pen and made an accurate calculation of the paths of the rays which fall on different points of a globe of water to determine at what angles after two refractions and one or two reflections they will come to the eye and then I found that after one reflection and two refractions there are many more rays which come to the eye at an angle of 41° to 42° than any smaller angle, and none which come at any larger angle. I found also that, after two reflections and two refractions there are many more rays which come to the eye at an angle of from

51° to 52° than at any larger angle and none which come at a smaller angle.

A Discourse on Method. Appendix III Les Meteores

Descartes' explanation of the primary and secondary rainbows did not include the role of colors. Isaac Newton, who was the first to explain the nature of colors (recall Chapter 1), explained the presence and order of the colors of the primary and secondary bows. He also greatly simplified Descartes' approach by using Calculus to derive a simple equation to find the rainbows' angles without needing to calculate the deflections of hundreds of rays.

"When you come to a fork in the road, take it." Yogi Berra

One well-known factor that determines the brightness of the rainbow is seldom mentioned in popular presentations. The rav approach of Descartes, colorized and improved by Newton still did not explain the intensity and brightness of rainbows. The problem occurs at every point the ray strikes the edge of the raindrop. There, the light comes to a fork in the road, so to speak, and takes it because some of the light is reflected and the rest is refracted.

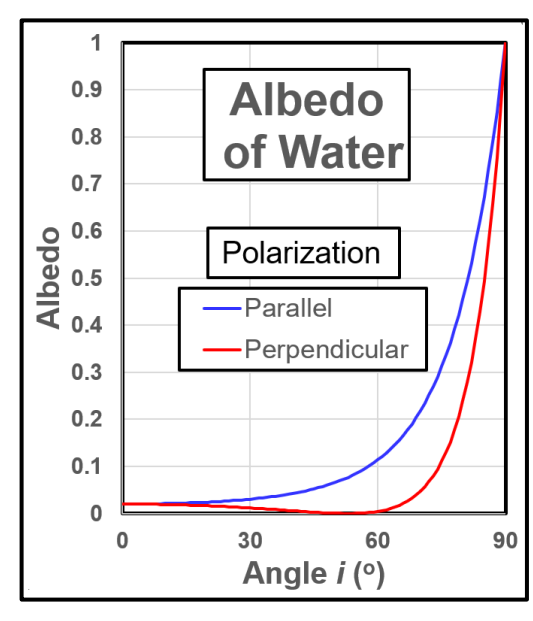


Fig. 9-17. Reflection fractions (albedo) of light passing between air and water. SDG.

In 1823, expanding on Young's finding that light consists of waves, Augustin-Jean Fresnel derived the two equations for the fraction of light reflected (i. e, albedo) at the interface between two different media such as water and air as a function of the angle of incidence, *i* (Fig. 9-17). There are two equations because light waves striking the

drop have two orientations (waves with electric fields either perpendicular or parallel to the drop's surface).

The percentage of reflected light remains small (< 10%) for each polarization when $i < 60^{\circ}$, after which it increases to 100% at $i = 90^{\circ}$. At $i \approx 53^{\circ}$, the so-called Brewster Angle, the albedo of the perpendicular component is 0. Light striking water at the Brewster angle is completely polarized. Since the primary rainbow forms near the Brewster at $i \approx 59^{\circ}$, where the albedo of the perpendicular component is only 0.35%, it is about 96% polarized.

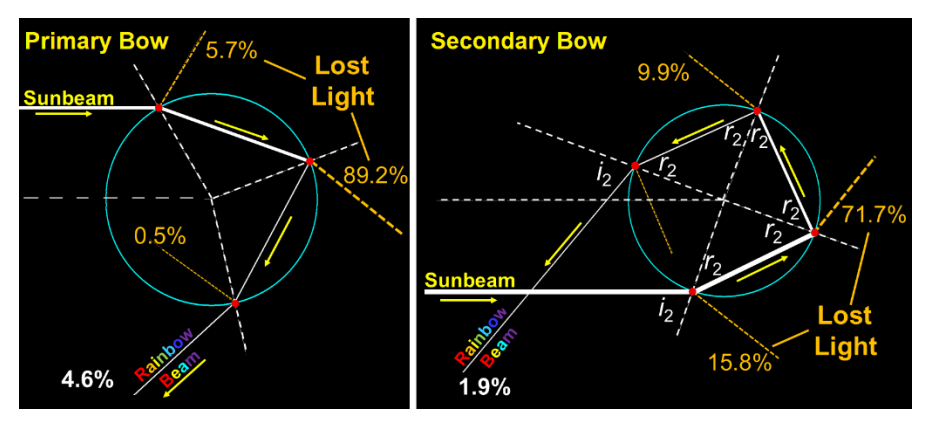


Fig. 9-18. Light beams that produce the primary (left) and secondary (right) bows and losses at each crossroad (red dots). SDG.

Fresnel's Equations brings us a giant step closer to evaluating the brightness of the primary and secondary rainbows. Fig. 9-18 shows the percent of light (the average of the two polarizations) lost or wasted at each fork and the final percent that contributes to each bow. The left panel shows the values for the primary bow. When the sunbeam strikes the drop only 5.7% is reflected or lost and 94.3% enters the drop. The largest loss to the bow occurs at the back of the drop where 89.2% of the initial light exits the drop. At the third fork, most of the remaining light, a measly 4.6% of the initial sunbeam (8.7% and 0.35% of each of the two polarized beams), forms the primary rainbow. If the back of the drop had acted like a perfect mirror the primary rainbow would be about 20 times brighter.

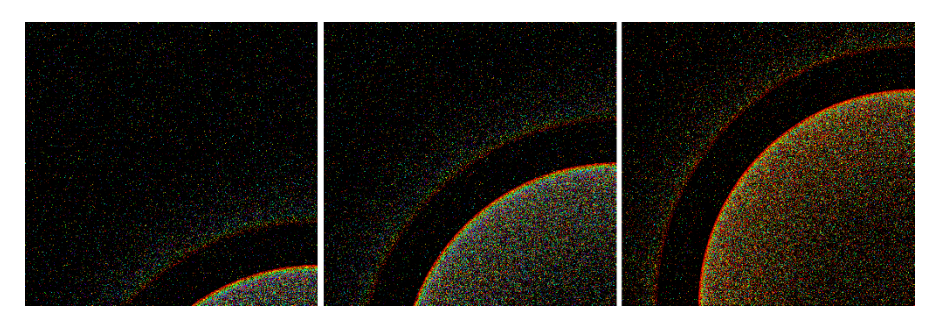


Fig. 9-19. Monte Carlo simulated rainbows for sun elevations 40° (left), 20° (center), and 1° (right) with dark background and no skylight. SDG.

The secondary bow's path and losses at each fork are shown in the right panel of Fig. 9-18. The incidence angle for the secondary bow is $i \approx 72^{\circ}$, and to produce a ray that heads down from raindrops in the sky to observers at the ground the initial sunbeam strikes the lower part of each drop. The secondary bow has four forks due to the additional internal reflection. With four forks for light to be lost, the secondary bow has only 1.9% the brightness of the initial beam.

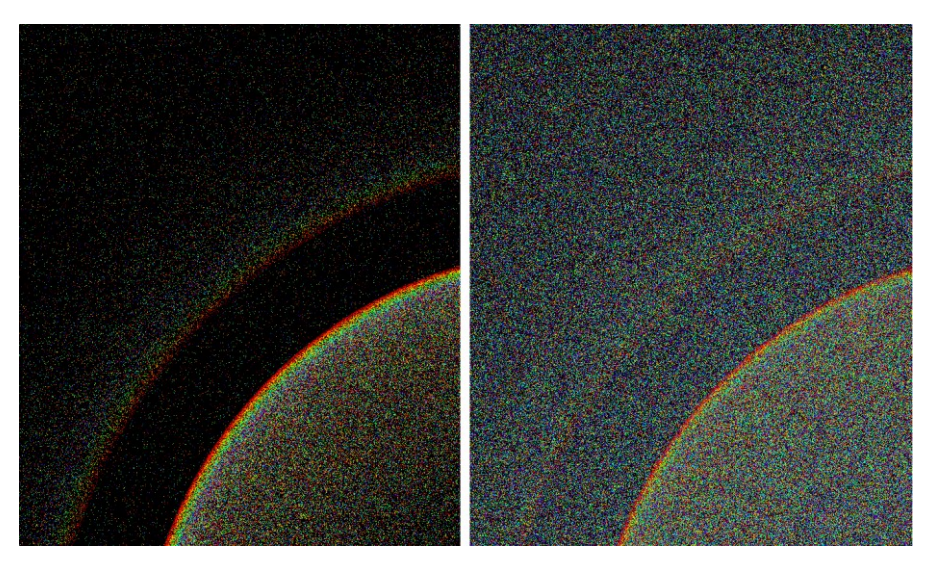


Fig. 9-20. Simulated rainbow for solar elevation 20° without (left) and with (right) skylight. SDG.

Rainbow simulations using the computer return to Descartes' cumbersome, lengthy Monte Carlo approach of calculating the results of aiming large numbers of beams at a raindrop. The Monte Carlo technique (briefly described in the Preface) can be pursued to any level of sophistication and detail. For the rainbow, the technique aims beams with the spectrum of Sunlight through the atmosphere where they suffer losses due to absorption and scattering. The beams hit all over the drop in random fashion. At each contact with the drop's edge Fresnel's equations determine the probability of reflection or refraction, and the laws of reflection and refraction determine the direction of the beams that ultimately leave the drop. The beams then are subject to scattering in the atmosphere on the way to the observer. Beams that reach the observer are recorded and mapped on the computer.

The three Monte Carlo simulations in Fig. 9-19 are done for rainbows that occur right in front of the observer after the beams pass through the atmosphere with an aerosol content that adds 20% to the optical thickness of the Rayleigh atmosphere at sea level with a black background at Sun elevations 40° , 20° , and 1° . In each case 5 million beams strike the drops.



Fig. 9-21. Reflected light from sunlit cumulus clouds brightens the glassy areas of the Caribbean Sea on 07 Dec 2014. SDG.

At each of the Sun elevations the primary bow stands out from the black background, and especially from Alexander's Dark Band, which is almost pitch black because drops scatter little light in that range. The right panel represents a reddened sunrise or sunset bow and the sky below the primary bow is also reddened. The secondary bow is fainter and wider than the primary bow in all three panels, the colors have lower purity, and they appear in the opposite order from the color sequence of the primary bow.

Including background skylight in the simulation, as in the right panel of Fig. 9-20, seriously vitiates the appearance of the simulated bows. The primary bow is still distinct, though with lower color purity but the fainter secondary bow is almost camouflaged. The main change is the brightening of Alexander's dark band by skylight.



Fig. 9-22. Early morning reflected sun glint from a building at the edge of the Port of Miami, FL on 12 Dec 2015. SDG.

The Fresnel reflection fractions have great significance in many natural phenomena and industrial products (e. g.,thin films) besides rainbows and halos. Their impact is especially important in climate. The albedo of water is quite low until the Sun is near the horizon, which is why water bodies look dark in satellite images and in most

photographs (except for sun glint). It also means that deep water absorbs sunlight with high efficiency, except when the Sun is near the horizon. The stratocumulus clouds that cover substantial areas of the east side of the subtropical oceans (recall Fig. 4-18 and Fig. 4-19) play a major role in cooling Earth's climate because they have much higher albedo than the ocean water below, and reflect much sunlight to space before it can heat the planet. The stratocumulus clouds also emit infrared radiation to space as if they were black bodies (and to infrared eyes, clouds do appear black) at almost the same rate as the ocean waters below them.



Fig. 9-23. Red waters of the Gulf of Mexico reflecting the light of twilight at Siesta Key, FL Dec 1987. SDG.

9.3 Rainbows to Reflect On

Reflection of light from normally dark water bodies has almost magical effects on rainbows.

Dark waters brighten and even gleam when light strikes it a glancing blow. In Fig. 9-21, the near glassy ocean reflects the white light from the sunlit side of cumulus clouds near the horizon (and even from the boat) except in the patches where the water surface is ruffled. Sun glint, even when reflected from the windows of a building (Fig. 9-

22), turns the normally dark waters blinding bright. When light near the horizon comes from sunset-reddened clouds (Fig. 9-23), the waters below reflect it and appear as if the Nile waters had turned to blood.



Fig. 9-24. A rainbow and its reflection in the water of Fairfield Lake, NC on 02 Sept 2018. SDG.

Rainbows are also reflected by smooth waters. After a thunderstorm chased everyone from the small beach on Fairfield Lake, NC late on the afternoon of 02 Sep 2018 the wind calmed in time to allow the smooth water to reflect the rainbow from the departing storm (Fig. 9-24). An oddity is that the rainbow we see reflected in the water is produced by different drops than drops producing the rainbow it appears to reflect. This is shown in Fig. 9-25, where the top of the flag and the primary rainbow both *appear* at the same height in the sky, but the flag's reflection *appears* lower in the water than the reflected bow because the primary rainbow beam always deflects light by 42°. Thus, the reflected bow is produced by drops lower in the rain shaft than the drops that produce the primary bow.

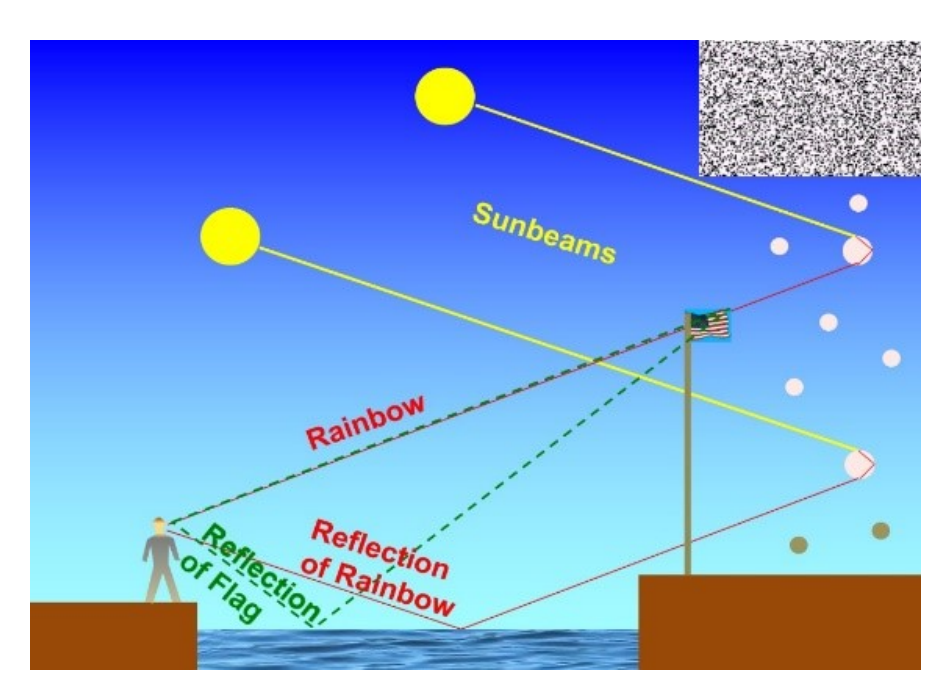


Fig. 9-25. The reflection of a rainbow in the water is produced by drops that are lower in the sky than the rainbow it appears to reflect. SDG.

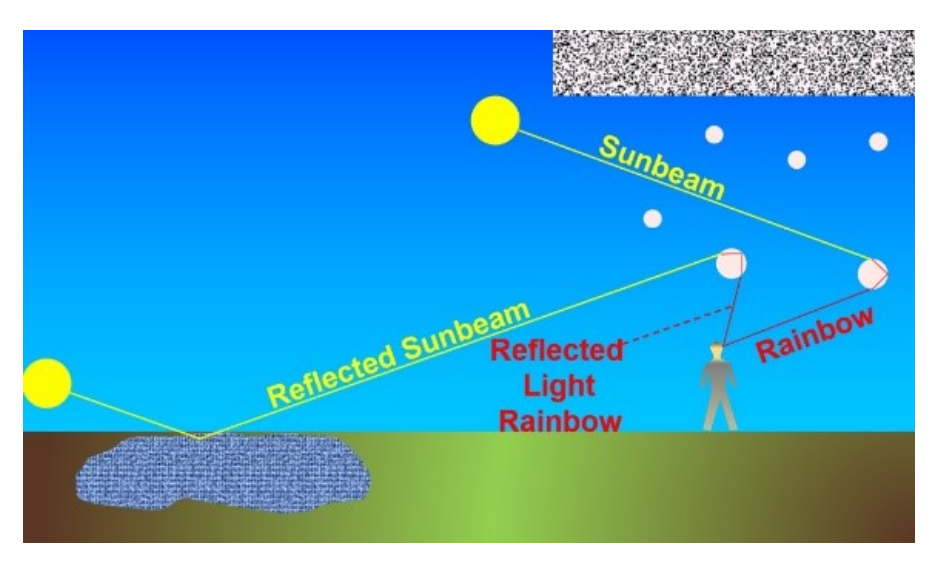


Fig. 9-26. Reflected light rainbows are produced by reflected sunbeams. The water surface mus be smpoth. SDG.



Fig. 9-27. A double rainbow and a double reflected light rainbow in Northern Ireland. ©William Bradley

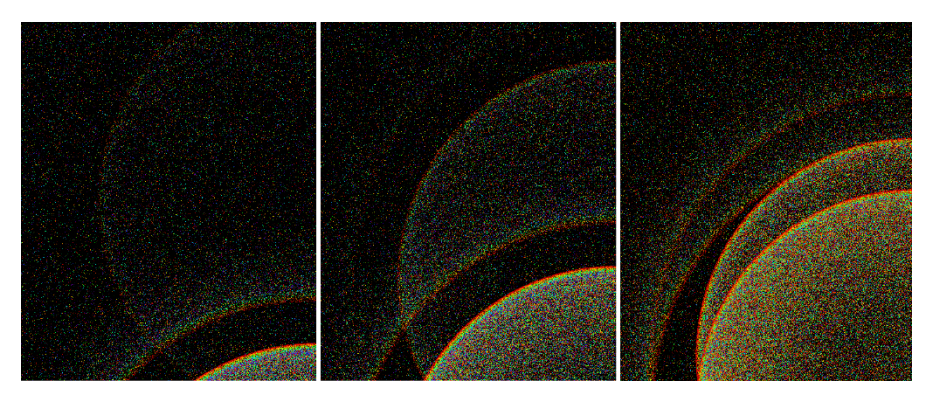


Fig. 9-28. Monte Carlo simulated rainbows and reflected light bows for Sun elevations 35° (left), 20° (center), and 5° (right) with dark background. SDG.

On rare occasions four rainbows appear in the sky. Imagine standing on the shoreline shortly before sunset, gazing out to sea facing the setting Sun. The sky over the sea is clear but rain is falling to the east from a shower. The sea is unusually calm and the sun glint in the water is almost as blinding as the Sun. You turn opposite the Sun to



Fig. 9-29. Twinned rainbow (top of primary bow) 21 Jun 2018 east of Cheyenne, WY produced by two different size populations of raindrops. Jan Curtis.

the rain in the east. Four rainbows tower in the sky. Attached like a siamese twin to the primary bow at the horizon, is a bow with the same color sequence but not quite as bright. Similarly, attached like a Siamese twin to the secondary bow at the horizon is another bow with its color sequence but not quite as bright. The Sun produced the primary and secondary bows. The Sun's reflection, not quite as bright but still a blinding, real light, produced the two extra bows. Such *reflected light rainbows* are illustrated in Fig. 9-26 and photographed in Fig. 9-27. The rainbows produced by the Sun form less than half circles if they are complete above the horizon. The rainbows produced by the Sun's reflection in the water form more than half circles if *they* are complete above the horizon and, spread outside the bows to which they are joined at the horizon.

All of the few photos of reflected light rainbows occur when the Sun is near the horizon. This follows from Fresnel's Equations of Reflection. Water reflects very little sunlight until the Sun is near the horizon, so the reflected light bow will be faint. For example, the albedo of water is only 4.4% when the Sun is 35° above the horizon, so reflected light bows will be less than 1/20th as bright as the normal bows even in the optimal case of mirror smooth water. When the Sun is 5° above the horizon the reflected light rainbow will be 13 times brighter because water's albedo is 58.4%. The Monte Carlo dot simulations of Fig. 9-28 illustrate this difference, where the reflected light bow is bright at Sun elevation 5° (right panel) but barely detectable, even with a black background at Sun elevation 35°. At Sun elevation 20°, where albedo is 13.4%, the reflected light primary bow is fainter than the normal secondary bow, so background

skylight almost completely swamps it, and even with a black background, the reflected light secondary bow is almost invisible.

9.4 Twinned and Disjoint Rainbows

The top of the arch of the primary bow in Fig. 9-29 is split, as if there were two primary bows, and indeed, there are. What is its cause? Up to this point we have assumed bows are produced by spherical drops. But large raindrops flatten on bottom, and when the drop flattens on bottom refraction, particularly for the exiting ray is altered so that the primary bow will flatten on top.



Fig. 9-30. Disjoint rainbow from sea spray and a fresh-water shower. Commissioned by Gunther Konnen.

If all the drops were the same size and were flattened or squashed the same way the bow would be squashed slightly in a manner particularly hard to notice. But when there are two distinct bows – twinned bows as they are called, it implies that the bows are produced by two distinct showers, each with different size drops, or

one shower with a split population of distinctly larger and distinctly smaller drops, in any case, a bimodal drop size distribution.

Twinned bows are always split at their tops and never on the sides where they are near vertical. That is because the rays that produce the vertical sides of the bow go through near horizontal cross sections of the drops, which are not squashed and remain circular.

A final rainbow oddity we consider here might be called a disjoint rainbow. Gunther Konnen reasoned that since salt water is denser than fresh water and has a higher index of refraction, its primary rainbow, like that of glass spheres, will appear closer than 42° from the antisolar point. He asked a mariner to look for a rainbow produced by a fresh water rain shower at the same time a rainbow was produced by sea water spray from the ship and photograph the scene. The seaman took the photo (Fig. 9-30) on his very next voyage, which confirmed Gunther's prediction.

9.5 Supernumerary Bows and Fog Bows: Waves

All the rainbows photographed up to this point in this chapter, are accurately described and modeled using geometric optics. But, as noted in Chapter 1, some rainbows have extra color bands just inside the primary called supernumerary rainbows. These bands add to the width of the primary bow and also embellish it. A beautiful example is the supernumerary bow of 21 Sep 2023, shown in (Fig. 9-31), which is a closeup of the double rainbow in Fig. 1-10. Jan noted it was,

"A crazy afternoon with slow moving and slow developing thunderstorms. This capture was taken in light rain as the thunderstorm passed to my east. The skies were clear to my back as the brilliant sunlight reflected and refracted off the nearby heavier rains. The supernumerary rainbow was as bright as I have ever seen. The secondary bow was surprisingly not as

bright as I would have thought. The primary bow was exceptional."

Light rain means small raindrops. Indeed, the best supernumerary bows and fog or cloud bows are produced in rain shafts or fog with small drops of almost constant size. How so?

Supernumerary rainbows and fog bows arise from the wave nature of light, As an example, consider two waves of length, $\lambda = 0.55 \, \mu m$ (corresponding to green) that strike a raindrop at the two different incidence angles, $i = 47^{\circ}$ and $i = 70^{\circ}$. Both these waves emerge from the drop at the identical angle from the antisolar point, 38.67° , but since they travel through different lengths both inside and outside the drop they will arrive at the eye out of phase, by an amount depending on the size of the drop. If the distance differs by half a wavelength then the two green waves will interfere totally and cancel so at 38.67° , the supernumerary bow or fog bow will have no green.



Fig. 9-31. Primary bow of 21 Sep 2023 at Oracle, AZ with pronounced supernumeraries, matched with Mie solution from Fig. 9-32 for drops with $r_{DROP}\approx 325~\mu m$ (extension at right). Jan Curtis.

These phase changes are almost random for large drops, which are more than 1000 times the wavelength of light, and hence have no impact on the rainbow. The phase changes and hence the color pattern become more consistent for succesively smaller drops. The supernumerary bows begin to appear for raindrops less than 1 mm in

diameter ($r_{DROP} = 0.5$ mm) and dominate increasingly for smaller drops while the primary rainbow becomes less colorful and distinct.

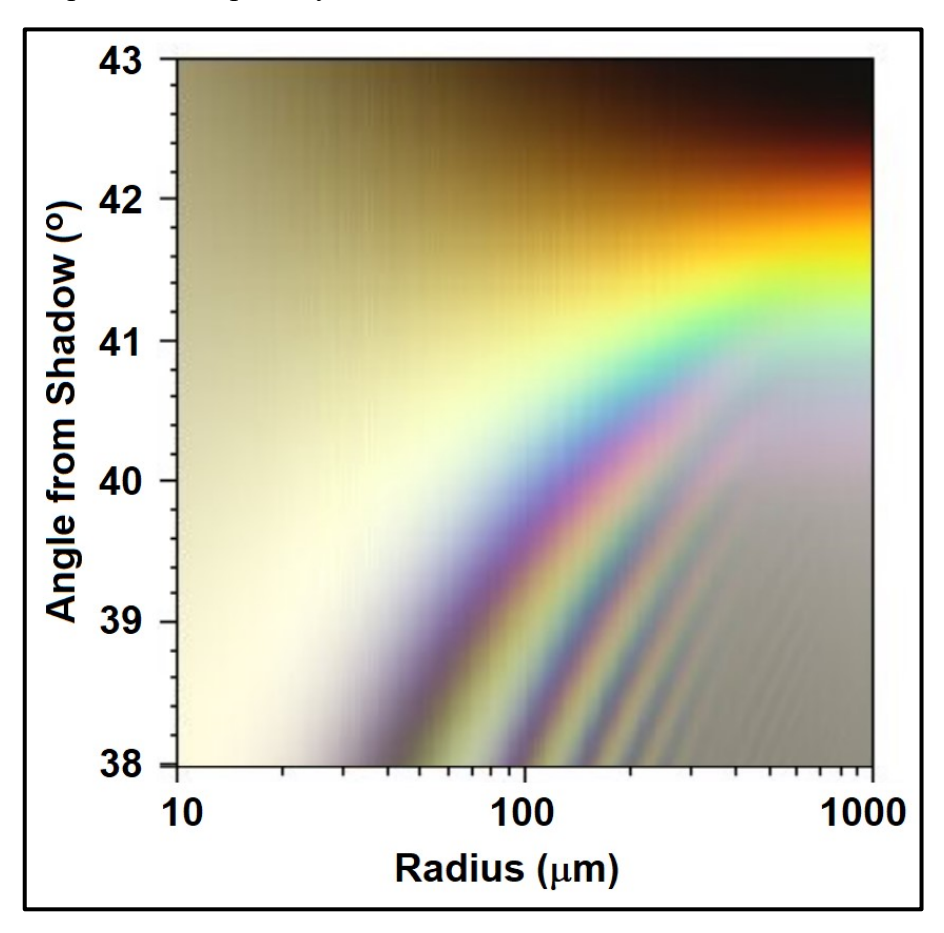


Fig. 9-32. Lee diagram of rainbow colors vs drop size and angle from shadow for a perfect Mie single scattering model. ©Phil Laven.

Ray Lee – that is Raymond Lee and not Lord Rayleigh – constructed a diagram using Mie scattering calculations that shows how the colors and deviation angles of the rainbow vary with drop radius. The Lee diagram for the primary rainbow and its supernumeraries is shown in Fig. 9-32 (calculated by Philip Laven using more than 24 hours of computer time (http://www.philiplaven.com/links2.html). Pretty as this Lee diagram is, it may be difficult to read at first, so it

makes sense to repeat it in Fig 9-33 by isolating three vertical stripes that correspond from left to right to small, medium, and large drops. Small drops ($r_{\text{DROP}} \approx 0.04$ mm) produce a wide, largely white fog bow or cloud bow with a few stripes of washed out colors and essentially no secondary bow. Medium size drops (($r_{\text{DROP}} \approx 0.2$ mm) produce multiringed supernumerary bows inside a broadened primary, and a wide secondary bow. Large drops (($r_{\text{DROP}} > 0.6$ mm) produce a bright, near spectral primary bow and a distinct secondary bow.

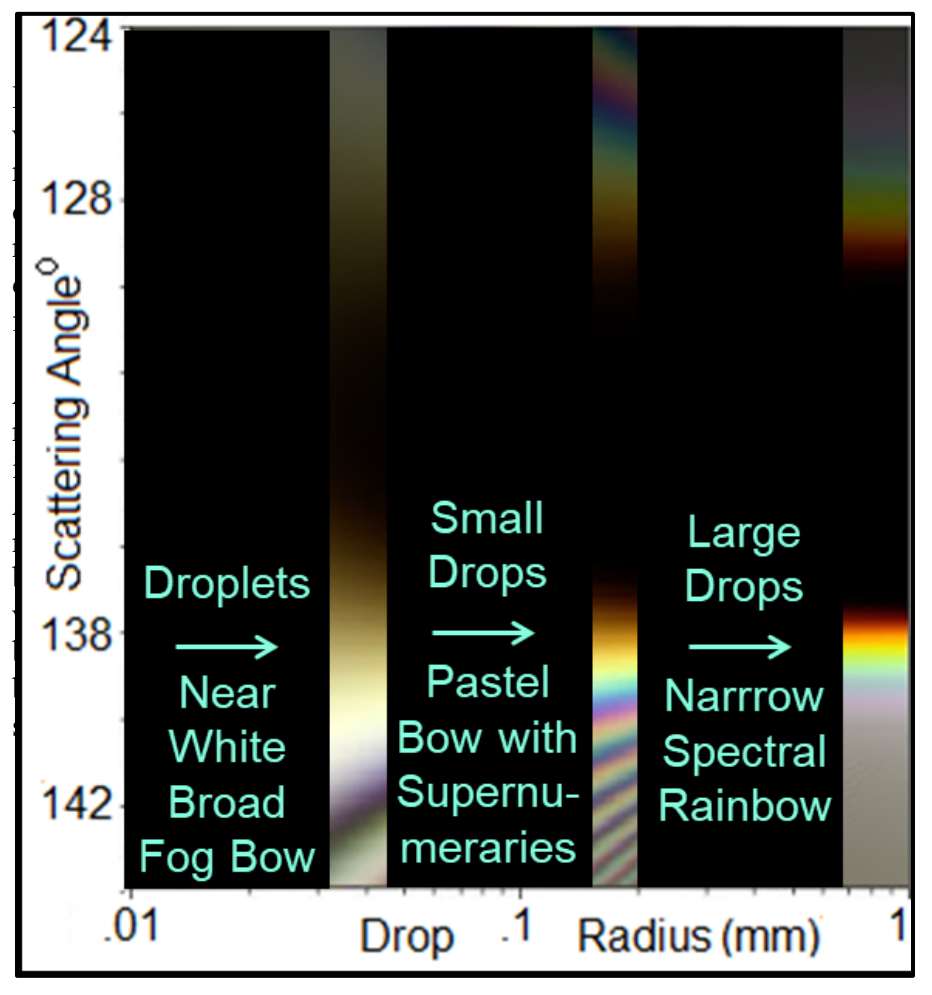


Fig. 9-33. Lee diagram showing drop-size regimes for fog bows, supernumerary bows and spectral primary bows. ©Phil Laven and SDG.





Fig. 9-34. Fog bows at Fenêtre sur le Saguenay, QB, Canada a few minutes apart on 13 Aug 2005. The darker background of the bottom panelbrings out the weak colors. SDG.

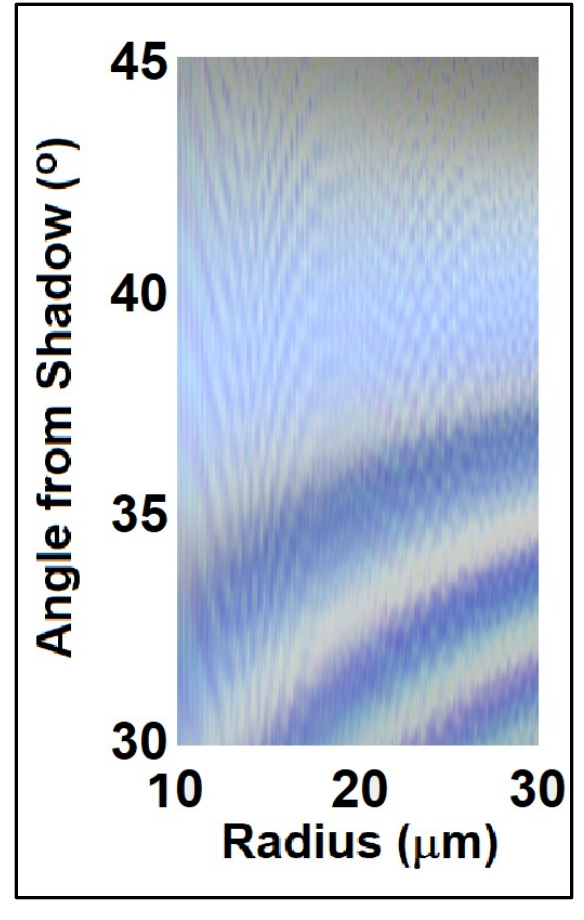


Fig. 9-35. Lee diagram for fog bows of small droplets. SDG.



Fig. 9-36. Fog bow in the Redwoods 31 May 2021. $\mbox{@Bill Young.}$

Matching photos of rainbows to vertical slices of the Lee diagram provides a way to estimate the

drop size. For example, the best match between the supernumerary bow of 21 Sep 2023, shown in Fig. 9-32, occurs for drops with $r_{DROP} \approx 325 \, \mu m$. The discrepancies between photo and model are due to the model's neglect of skylight and the range of drop sizes that always occurs in any rain shaft or fog.

Anyone who sees a fog bow for the first time after having seen many rainbows is struck by the difference. The fog bow shown in the top panel of Fig. 9-34 lit up in stunning fashion as fog and drizzle began clearing around 1630 ADT on 13 Aug 2005 at Fenêtre sur le

Saguenay, QB, Canada after a miserable, raw, rainy and windy day. It consisted of two very broad, almost blinding bright white bands with total width about 10°, compared to the 2° width of the geometric optics primary bow. The faint color sequence became more distinct a few minutes later (in the bottom panel of Fig. 9-34) when seen with a background of a dark, forested hillside. Its color sequence, the opposite of the primary bow, puzzled Stan until he matched it to the color sequence and width of cloud bows made by droplets with $r_{\rm DROP} \approx 18~\mu{\rm m}$ in the Lee diagram of Fig. 9-35. Note that tiny variations of droplet size (which Nature always provides) are needed to eliminate the fine scale variations of the Mie scattering solutions of Fig. 9-35.

The most beautiful photo of a fog bow that we've ever seen (Fig. 9-36) is the one Bill Young captured one morning in the Redwood

forest. There, the very limited sunlit space provided optimal

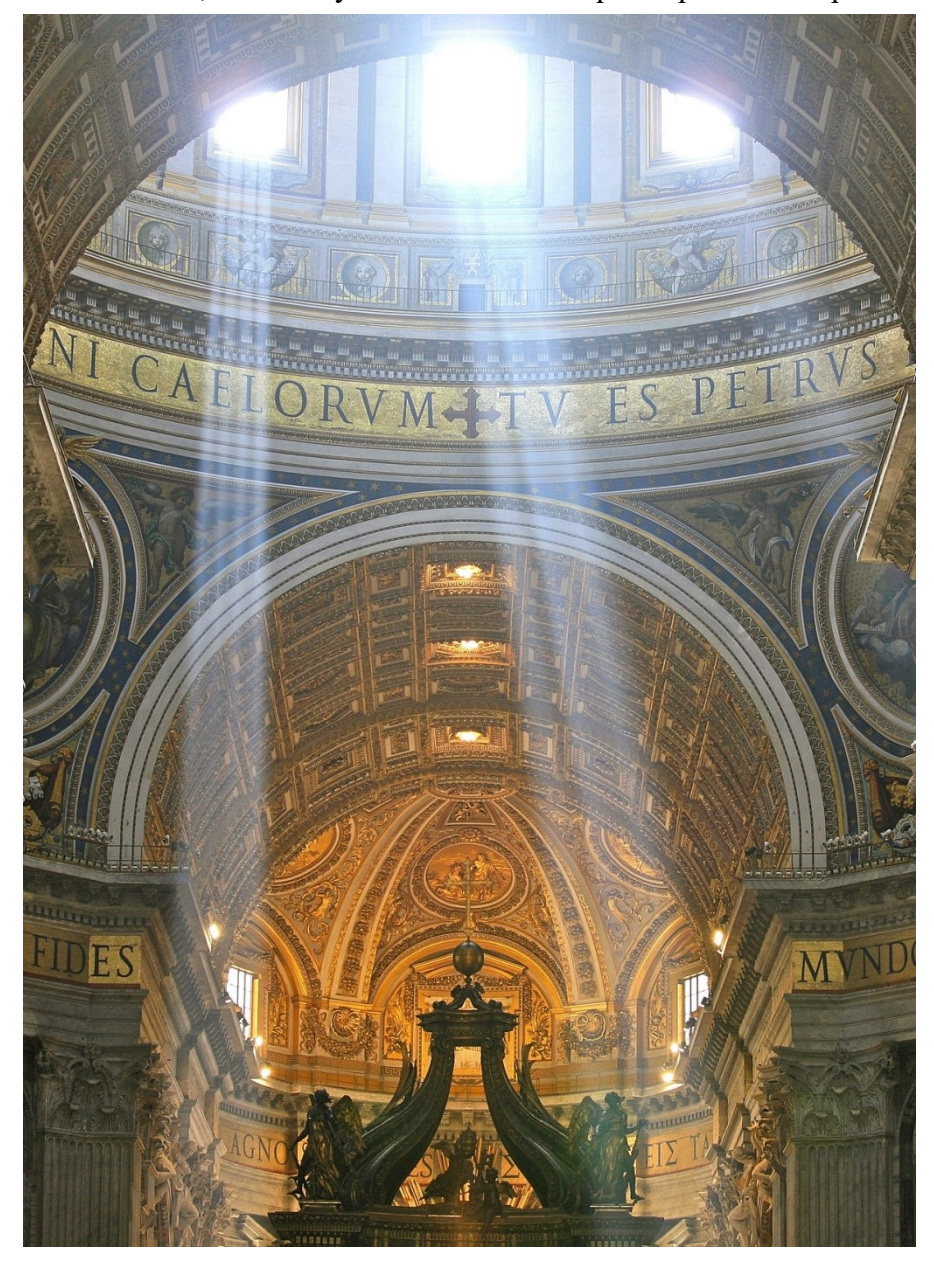


Fig. 9-37. Crepuscular rays, a divine symbol, shine through the windows of the dome in St. Peter's Basilica, Vatican City. Inside air quality is suspect, or perhaps the humidity is high. ©Alex Priomos..

conditions for uniform droplet size, which we estimate from comparison with the Lee diagram of Fig. 9-35 to have radius, $r_{DROP} \approx 27 \mu m$. And in a precious few minutes the Sun evaporated the fog droplets and the bow was gone.

9.6 Crepuscular and AntiCrepuscular Rays

By placing gods in the sky, ancient religions attributed atmospheric optical phenomena to divine sources. Foremost among these are crepuscular rays, which appear to emanate from the Sun, sometimes beaming down to reveal sanctity, as in St. Peter's Basilica (Fig. 9-37), and sometimes spreading in all directions (Fig. 9-38).



Fig. 9-38. Crepuscular rays emerging in all directions from the Sun on 16 Jun 2020, east of Cheyenne. Smoke from numerous Western US forest fires embellished the rays and allergies. Jan Curtis.

What causes crepuscular rays and what gives them their appearance? An impressive demonstration illustrating the nature of crepuscular



Fig. 9-39. Crepuscular ray from sunlit smoke of a BBQ grill. SDG.

rays is to aim a laser beam across a dark room. Nothing can be seen except for a red dot at the point on the wall the beam strikes. But the beam suddenly lights up the moment chalk dust or flour is sprinkled along it. Crepuscular rays can also be seen when a shade is opened a mere slit in a dark room. In that case, you can see individual dust particles light up. Smoke from barbeque grills also works (Fig. 9-39).

Crepuscular rays are sunbeams illuminated by dust, aerosol particles or air molecules that scatter light toward some observer.

They appear by contrast with shaded regions of the atmosphere; in fact, sunlit and shaded crepuscular rays often alternate. Opaque clouds that provide dark shadows but only cover part of the sky, such as cumulus or cumulonimbus clouds are usually the objects that cause the shade, but mountains or trees also work.

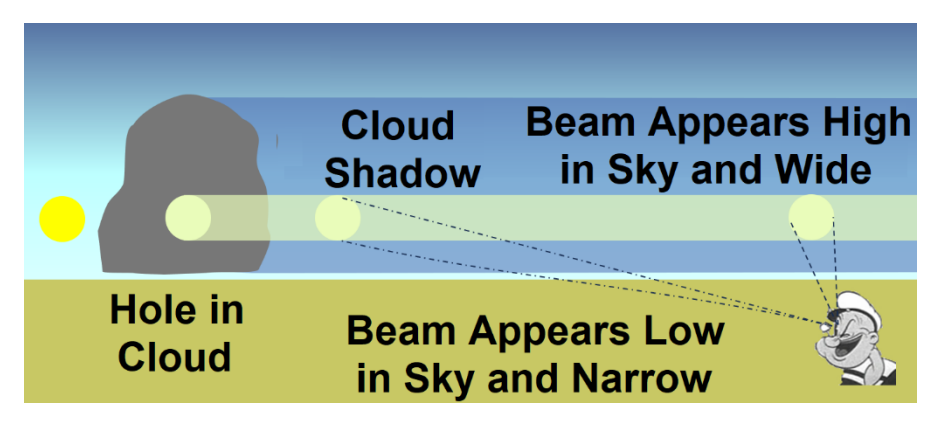


Fig. 9-41. When the Sun is at the horizon a horizontal sunbeam passing through a hole in a cloud produces a crepuscular ray that appears to spread as PopEYE looks higher in the sky. SDG.

The apparent spreading of crepuscular rays in all directions confounds their reality since sunbeams are all almost parallel and only aim downward during the day unless reflected in the water. A diagram of the astronomical setting illustrates why the Sun's rays are almost parallel. In Fig. 9-40 everything is drawn in proportion except

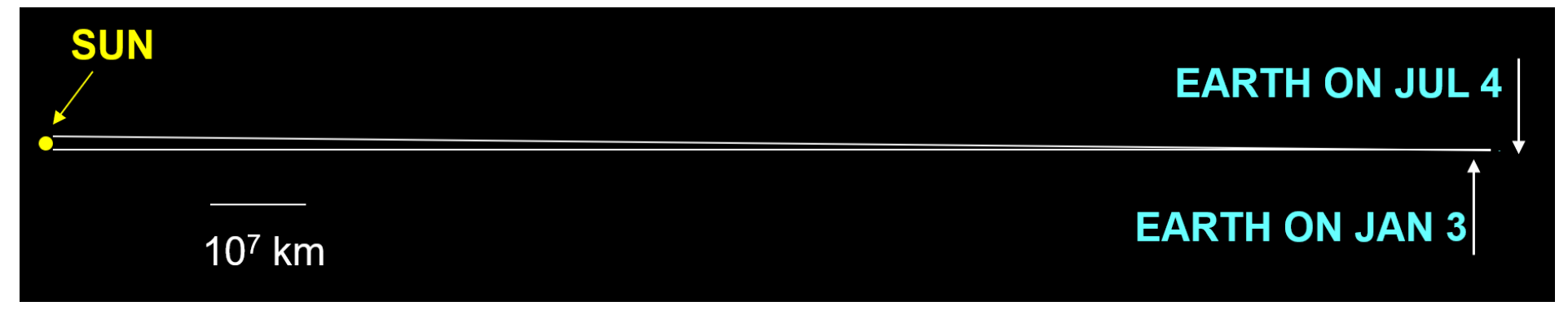


Fig. 9-40. Relative size of the Earth, Sun, and the distance between them. Sunbeams reaching Earth are all almost parallel, varying by a maximum of 0.53°. SDG.

that the almost invisible blue dot (just to the right of where the sunbeams converge) representing the Earth is 15 times too large! The Sun, whose diameter is 1.4 million km or 108 times the diameter of Earth, appears to us a tiny circle in the sky, only 0.53° wide, because it is so far away, an average of 149.5 million km. As a result all sunbeams reaching Earth at any moment differ by a maximum of 0.53°.



Fig. 9-42. Parallel crepuscular track rays and parallel altocumulus cloud bands at sunset in Granada, Spain on 11 Oct 2007 appear to converge in the distance because of linear perspective. SDG.

Fig. 9-41 illustrates how crepuscular rays appear to diverge from the Sun in all directions. It shows the Sun at the horizon with a distant cumulus cloud blocking its rays except for one hole in the cloud that allows the horizontal sunbeam through, which passes directly over the observer. The part of the beam near the cloud appears low in the sky. It is much further from the observer than the part of the beam directly overhead, so, by linear perspective, it appears to broaden with elevation angle. The samel illusion of broadening due to perspective is illustrated by train tracks, which we know are parallel, narrow in the distance, as at the Train Station in Granada Spain at sunset on 11 Oct 2007 (Fig. 9-42), which also contains parallel bands of altocumulus clouds seeming to narrow in the distance.



Fig. 9-43. Crepuscular rays at the edge of a cumulonimbus cloud Cheyenne, WY 15 Jul 2023. Rays are brighter at right center, near the Sun. Jan Curtis.

Crepuscular rays can appear faint or striking depending on the cloud's optical thickness and on the quantity and character of the aerosol particles. Cumulus and cumulonimbus produce crepuscular rays with the greatest contrast between light and dark rays, as in Fig. 9-43, Fig. 9-44, and Fig. 9-45, because they are so optically thick almost no light penetrates them and hence they cast the darkest shadows. Optically thinner and smaller clouds such as the delicate

cells and ripples of altocumulus, allow more light through as in Fig. 9-46, and so, tend to produce faint and fine crepuscular rays.

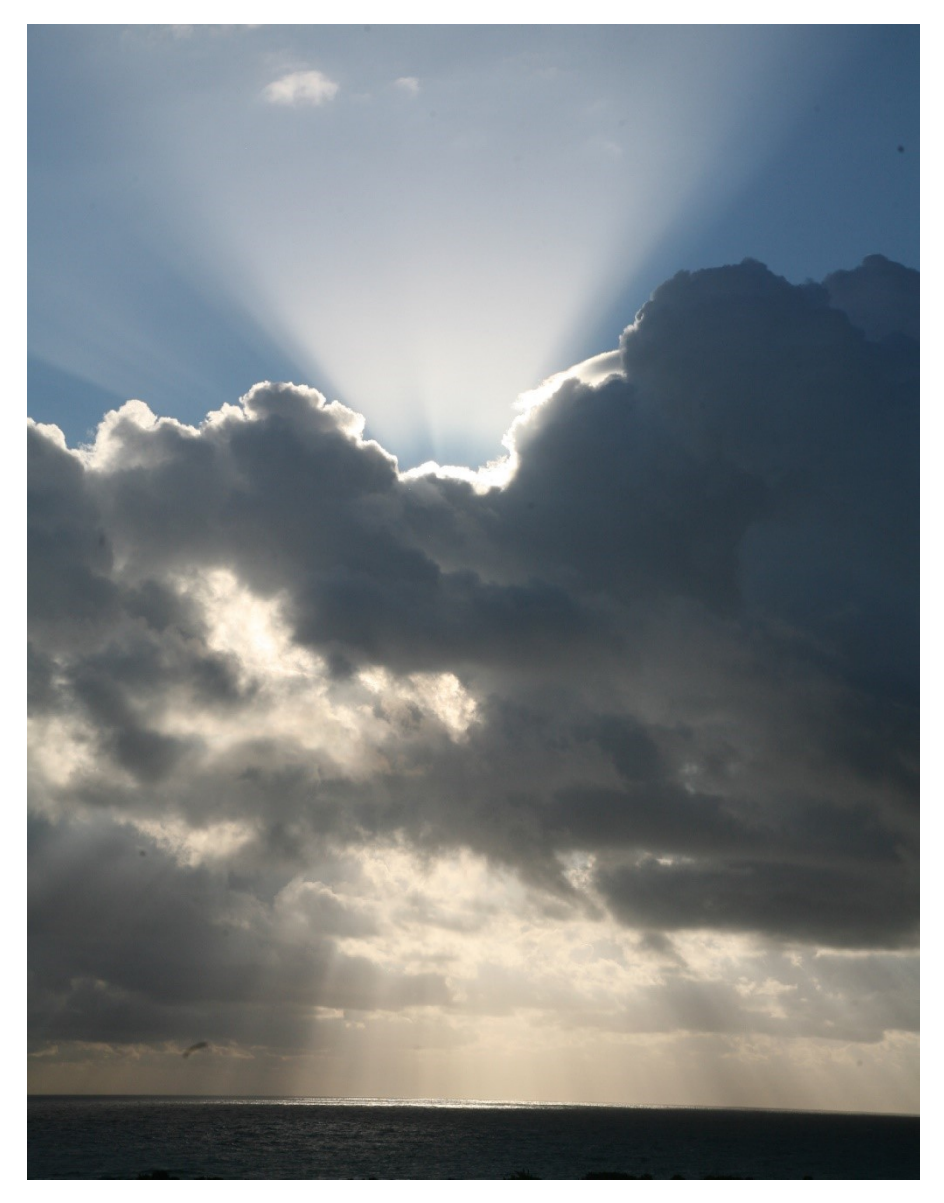


Fig. 9-44. Crepuscular rays from Cu illuminate the humid morning air and the distant sea surface, 20 Dec 2011, Fort Lauderdale, FL. SDG.



Fig. 9-45. Crepuscular rays beaming through a hole in a field of cumulus in Cliffside Park, NJ. SDG.



Fig. 9-46. Crepuscular rays from a sheet of altocumulus cloud cells in smoky air, 17 Jul 2017, east of Cheyenne, WY. Jan Curtis.

A purely molecular atmosphere tends to produce feeble and blue crepuscular rays. Add aerosols from pollution, fires, or airborne dust from distant dust storms, swell them in high humidity and perhaps even add fog droplets in the morning mist, and crepuscular rays light up. Impressive crepuscular rays in the dry air of Wyoming, as on 15

Jul 2023 (Fig. 9-43), are more likely due to dry smoke particles from forest fires. Impressive crepuscular rays in the SE United States are more likely due to aerosols bloated by deliquescence in humid air (Fig. 9-44, Fig. 9-47).

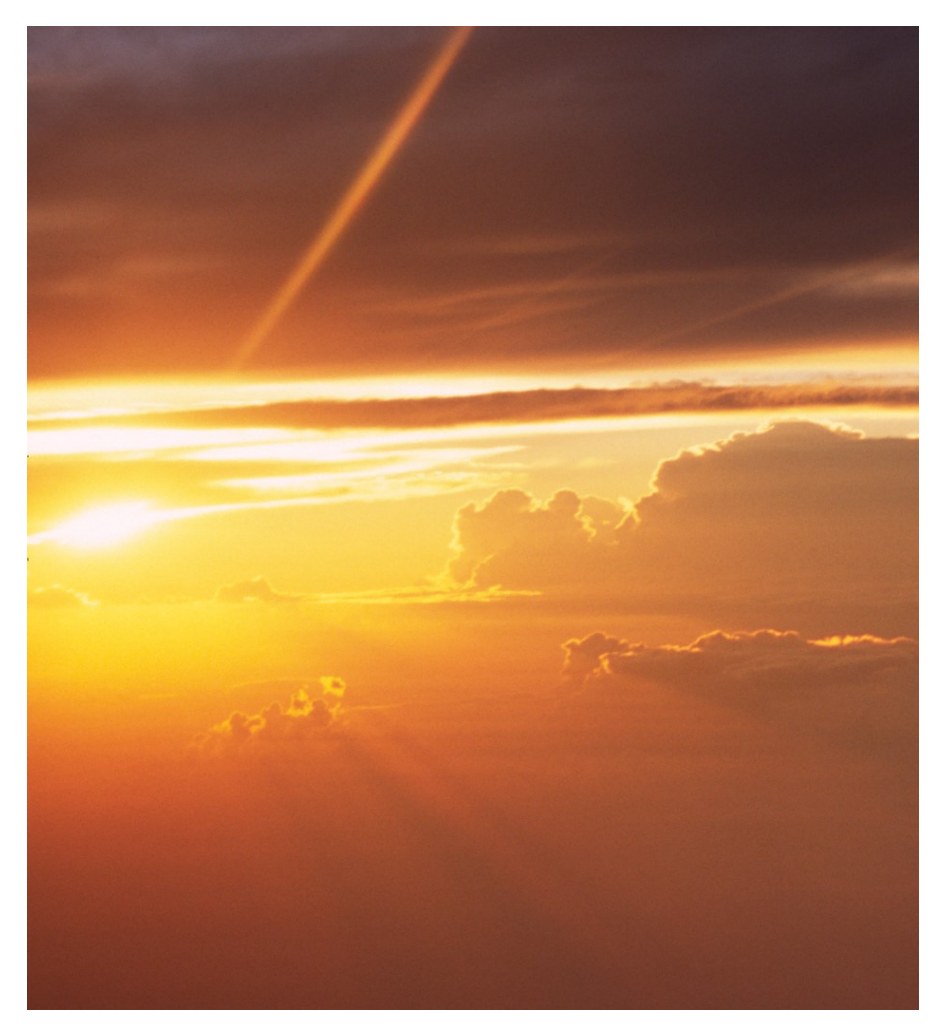


Fig. 9-47. Golden crepuscular ray searchlight beam at sunrise flying north over Florida. SDG.

Crepuscular rays tend to fade with angular distance from the Sun because most aerosols scatter light by small angles with much greater efficiency than by large angles (Recall Fig. 1-16, Fig 2-21 and Mie

scattering). For the same reason, the aerosols on dirty windshields produce a blinding and hence unsafe glare when facing the Sun, but not when lit from behind.

The principles governing crepuscular rays may be simple but their variations are prolific. They result from all the different sizes, opacities, and shapes of the clouds (or other obstacles including mountains), each with with unique, multiple indentations, evermoving around the ever-moving Sun, and endless variations of the atmosphere's aerosol content, concentration, and distribution. For example, the crepuscular rays of Fig. 9-43 that emerged from the side of a cumulonimbus cloud are bright where the edge is close to the Sun and deep blue where it is far enough away to cast a wide shadow in relatively clean air. Time lapse videos show crepuscular rays moving like searchlight beams, as openings in the cloud move and change, and as the Sun moves. One example, for sunlight beams, is,

https://www.flickr.com/photos/cloud_spirit/51426097845/in/album-72157673641455795

Crepuscular rays at twilight (crépusculaire means twilight in French) take on twilight colors (Fig. 9-47) and sometimes surprising color contrasts On 16 Aug 2021 (Fig. 9-48) the rising sun, surrounded by a red glow, peeps beneath a distant cumulonimbus cloud that casts a blue crepuscular ray shadow in the otherwise reddened sunlit sky.

The color and lighting differences of twilight crepuscular rays can be simulated, as in Fig. 9-49. In the simulation, two major tricks were used and one major assumption was made. Trick #1: A skylight model was run twice – once to produce an image for a clear twilight sky and once for a beam shaded by a distant, towering thunderstorm. Trick #2: A widening wedge of the shaded beam (to mimic perspective) was grafted into the clear sky image to match a photograph taken during twilight. The assumption: no light from the sunlit sky was allowed to be scattered into the shaded beam and then scattered again to the observer. That assumption was validated both by calculations and by similarity between the photo and the simulation.



Fig. 9-48. A blue crepuscular ray shaded by a cumulonimbus cloud contrasts with a bright orange sky east of Cheyenne, WY moments after sunrise, 16 Aug 2021, with Air Quality Index = 100 (borderline polluted). Jan Curtis.

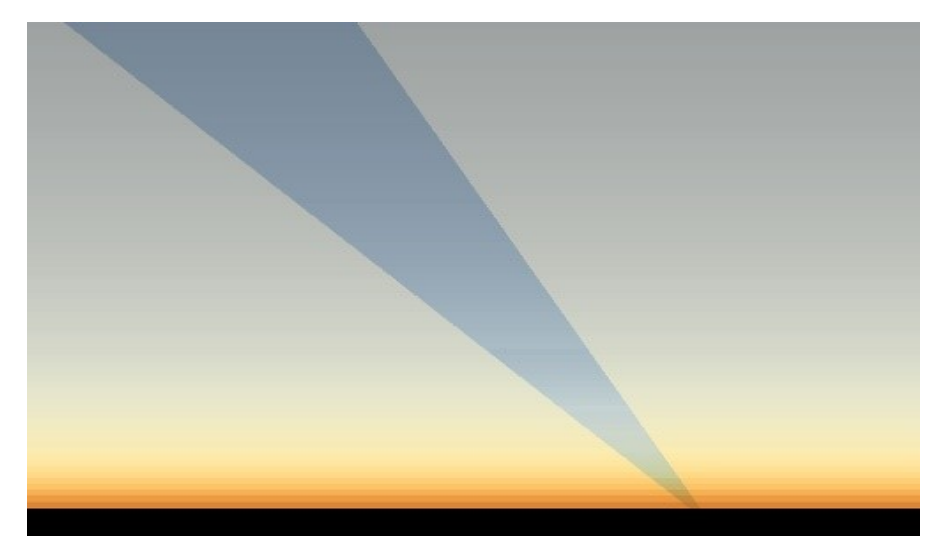


Fig. 9-49. Simulated crepuscular ray at twilight (Sun elevation = -1.8° produced by a distant cumulonimbus cloud. SDG.

Fig. 9-50 illustrates why the shaded beam is bluer and darker than the surrounding atmosphere. The unshaded beam (the white line in the

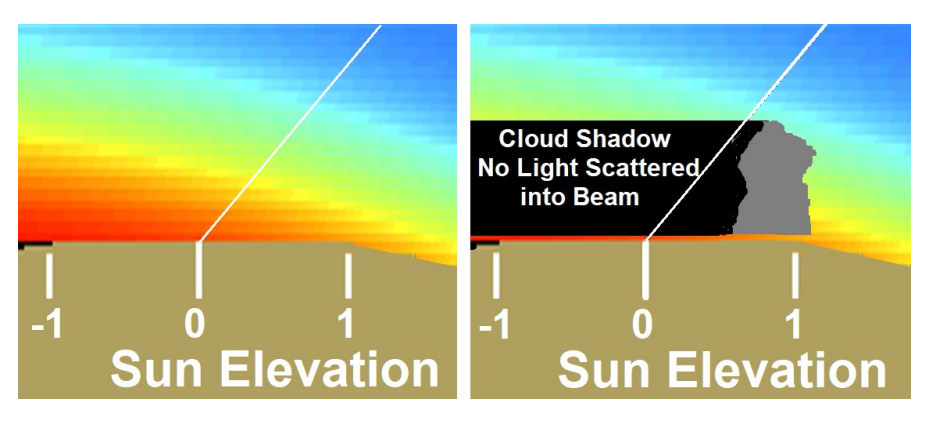


Fig. 9-50. Beam in clear air includes scattered sunlight from all heights in the atmosphere and therefore much red light from the lower troposphere. Beam shaded by a towering cumulonimbus only includes blue light from the upper troposphere. SDG.

left panel) receives light scattered from the top of the atmosphere all the way to the ground. (recall Fig. 2-12). When the Sun is at the horizon that includes a large contribution of red light. The beam in the shadow only receives light scattered from the top of the atmosphere to the top of the cloud shadow. That light is primarily blue beause high in the troposphere, where the atmosphere is thin, the scattered sunlight is still blue.

A walk through the woods in the early morning mist often reveals crepuscular rays, where instead of towering clouds, the trees and leaves form the obstacles (Fig. 9-51). On rare occasion, the droplets in the mist or ground fog will all be almost the same size, and in that case, the rays become iridescent.

Shortly after dawn, the crepuscular rays produced by trees can exhibit color variations normally produced by distant mountains or towering cumulonimbus clouds. On the morning of 18 Oct 2024 rays of the rising Sun peered through gaps in the forest around Fairfield Lake, NC near the bottom of Fig. 9-52. The sunlit rays, as well as the sunlit sky above were pink because the sunlight scattered by the low lying radiation fog overwhelmed the light of the blue sky above. By contrast, the shaded rays in the sky immediately above the fog-

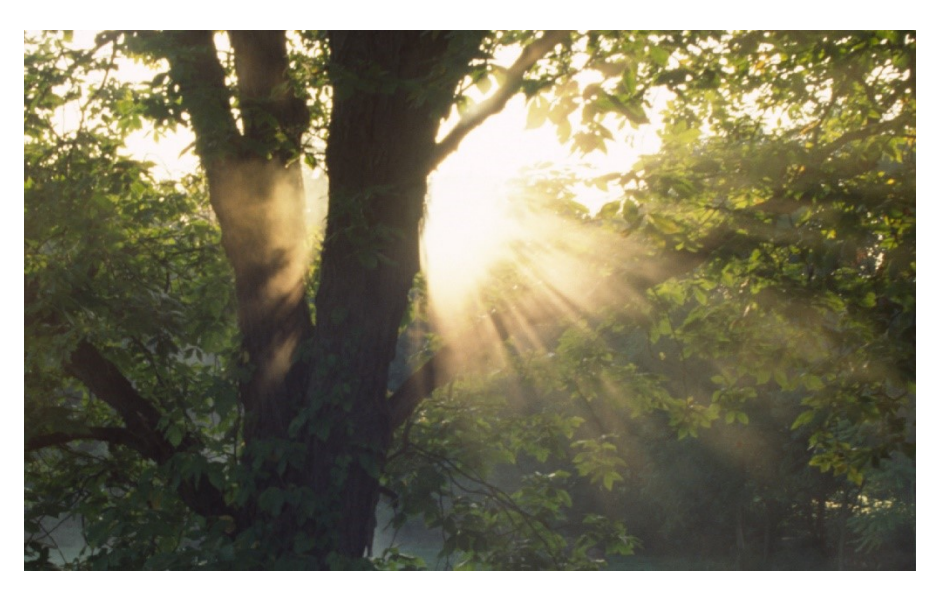


Fig. 9-51. Crepuscular rays through foliage in morning mist USR NJ. SDG.

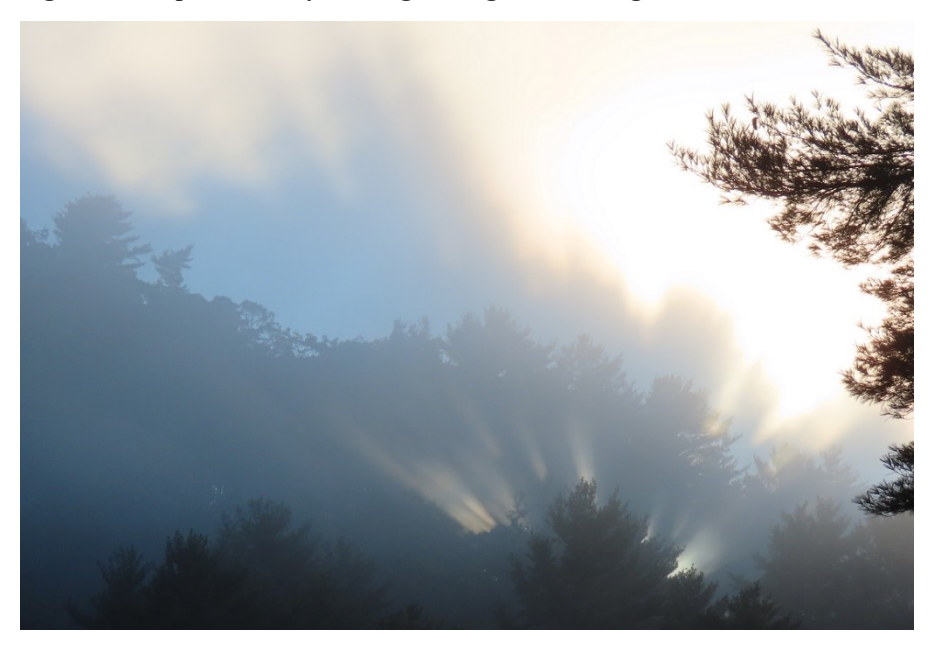


Fig. 9-52. Crepuscular rays from the rising Sun appear through and above the forest, whose treetops emerge above a thin layer of radiation fog at Fairfield Lake, NC 18 Oct 2024. SDG.

dimmed treetops were sky blue because they suffered no



Fig. 9-53. Crepuscular rays copy a cumulus outline onto a low haze layer, Boynton Beach, FL 29 Dec 2015. SDG.

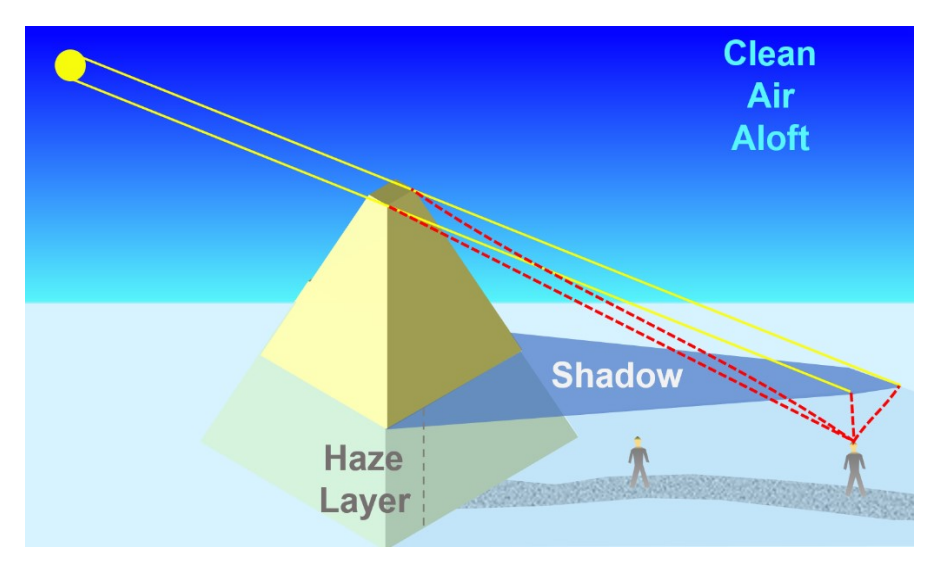


Fig. 9-54. Crepuscular copy rays of a mountain on a shaded haze layer. SDG. competition. A perhaps subtle feature of the blue shaded rays is that they traced out the outlines of the treetops.

Some crepuscular rays make almost perfect copies of the outlines of the clouds (Fig. 9-53), mountains, or trees whose shade caused the rays. These shaded copy rays often appear bluer by shading the bleached aerosol layer, and higher in the sky than the objects they copy by perspective, adding a sense of astonishment.

Shaded crepuscular rays that copy the object yet appear above it makes sense by recalling that when the Sun is above the horizon even its rays that pass overhead always aim downward. The copy image is often caused when the shadow-producing clouds or mountains or trees puncture a humid or dusty, aerosol laden air layer near the surface and rise into clean, dry air above. They then cast mimicking shadows, much like an impression of the cloud or mountain outline, on the top of the humid layer below, as on a screen. This is illustrated in Fig. 9-54.

When crepuscular rays reign turn your eyes to the opposite side of the sky from the Sun. There you may see *anticrepuscular* rays, which are crepuscular rays seen on the opposite side of the sky from the Sun and by perspective converge at the antisolar point.

A unique anticrepuscular ray, produced by the exhaust cloud of the Space Shuttle Atlantis shortly after the launch of NASA Mission STS-102 at 1832 EST on 07 Feb 2001, was photographed by Patrick McCracken (Fig. 9-55). Since sunset was 1807 EST, this was a twilight photograph, with the lower part of the exhaust cloud (and atmosphere) in Earth's shadow. Direct sunlight illuminated the upper part of the cloud, with red light from sunbeams that skirted just above the horizon, grading through yellow to white as sunbeams passed through thinner air aloft to reach the cloud. The shaded, dark blue ray aimed at the antisolar point but also appeared to aim at the Moon. This was a case of serendipity because it was a Full Moon, the only time the Moon is at or near the antisolar point.

On occasion the anticrepuscular rays will cross rainbows, combining two ancient symbols of aerial divinity in a single scene. Such a scene was first ilustrated by Luke Howard. Anticrepuscular rays always cross the primary and secondary bows at right angles, like spokes on a wheel, as in Fig. 9-2, Fig. 9-56 and Fig. 7-13. The rays often extend from bright or dark spots on the bow.



Fig. 9-55. Anticrepuscular ray as the shadow of the exhaust cloud of Space Shuttle, Atlantis 1832 EST 07 Feb 2001, NASA STS-102. The rays seem to point to the Moon only because it is a full Moon, which always appears opposite the Sun. Patrick McCracken.



Fig. 9-56. Spoked double rainbow with anticrepuscular rays over Cheyenne, WY, 08 Jun 2024 (recall Fig. 9-1). Jan Curtis.

Anticrepuscular rays are not seen often in the Eastern United States in part because the horizon is often blocked, but they are surprisingly common and sometimes quite dramatic under open skies from the Great Plains west. Like crepuscular rays, they change constantly as the clouds and Sun move, as on 30 Apr 2018 (Fig. 9-57), when, as

Jan noted, "Against the backdrop of a departing thunderstorm, the Sun broke through a gap in the clouds and the sunbeams were crazy for about 5 minutes". The video of the rays can be seen at,

 $\frac{https://www.flickr.com/photos/cloud_spirit/26948984667/in/album-72157673641455795/$



Fig. 9-57. Anticrepuscular rays seconds apart, 30 Apr 2018 at Cheyenne, WY. Jan Curtis.

Anticrepuscular rays can also take on the colors of sunrise or sunset, as in fig. 9-58 just before sunset on 14 Oct 2016 when the dimly lit house shows the scene faces opposite the setting Sun.

At times it is difficult to know if you are seeing crepuscular rays or rain fallstreaks. Fig. 9-59 has the virtue of showing both. At other times, the obstacles producing the rays are out of sight, perhaps

beyond the horizon, as in the twilight rays in the dust-filled stratosphere on 07 Sep 2019 (Fig. 9-60). Such twilights were produced for months following the eruption of Raikoke (one of the Kuril Islands east of Siberia) on 22 Jun 2019, as its tiny aerosol particles filled the stratosphere, and with no rain or snow to wash them out fell at a snail's pace.



Fig. 9-58. Colorful sunset anticrepuscular rays, Cheyenne, WY, 14 Oct 2016. Jan Curtis.



Fig. 9-59. Crepuscular rays crossing rain fall streaks, 04 Sep 2023, Cheyenne, WY. Jan Curtis.

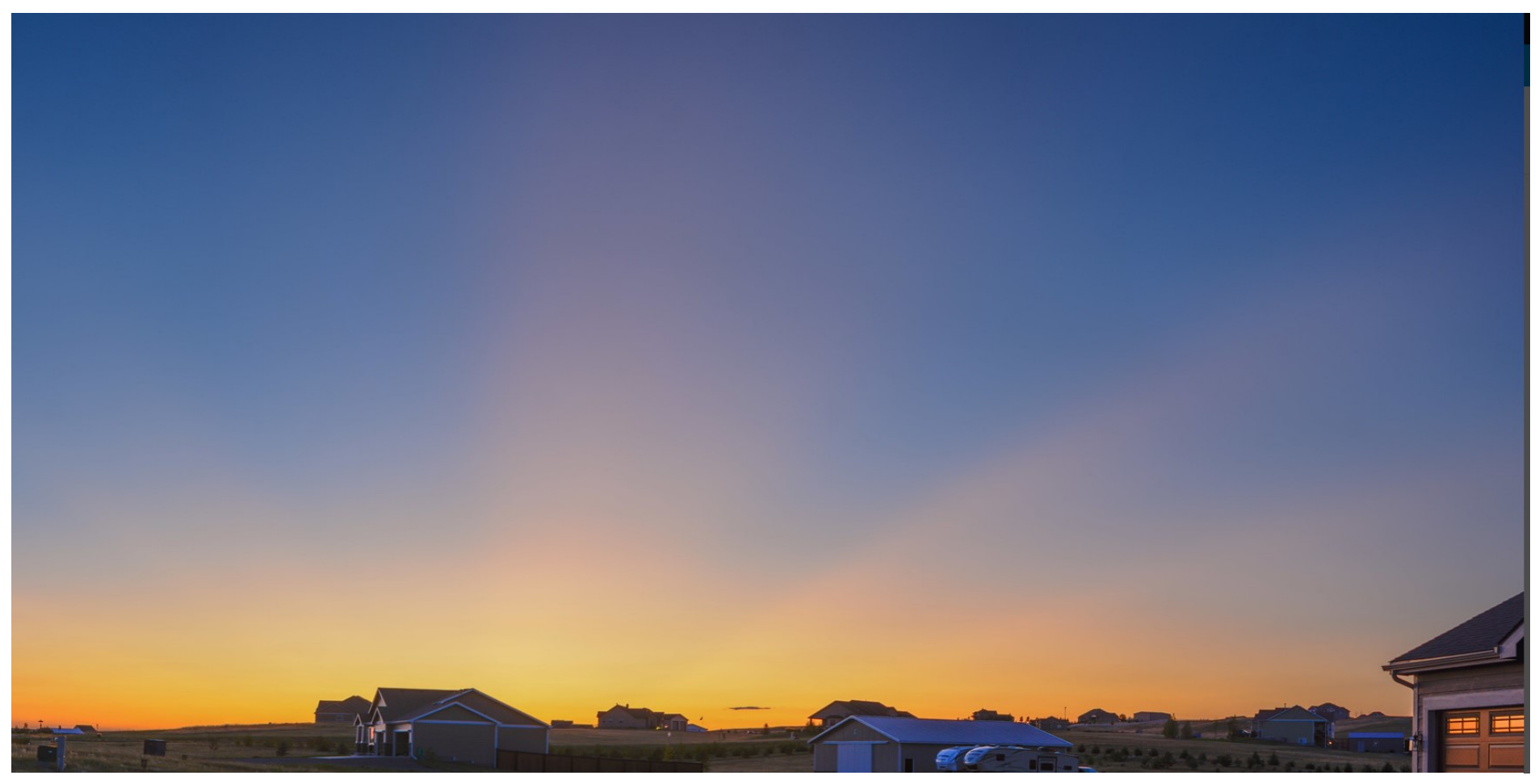


Fig. 9-60. Crepuscular rays after sunset over Cheyenne, WY, 07 Sep 2019 from ash of the Raikoke Eruption of 22 Jun 2019. Jan Curtis.

9.7 Hotspots and the Heiligenschein

A curious feature, often called a hotspot, is the bright area on the ground just above the apex of the shadow of the house in Fig. 9-61 (a close-up view of Fig. 9-57). The enhanced brightness of the ground at the antisolar point is a common observation on dry ground. It occurs because all shadows of the ground cover lie hidden directly behind the objects. At any other angle, some fraction of the shade of objects appears, with the effect of darkening the ground.

A different type and cause of brightening occurs at and around the antisolar point when dew is on the grass or other vegetation. The *heiligenschein* (holy glow)is due to sunlight backscattered from sparkling drops of dew in the morning The drops resting on the hairs of the grass or on waxy leaves act as retroreflectors (as in paint on street lines and road signs), reflecting sunlight directly backwards with increased focus. (Fig. 9-62).

The Renaissance goldsmith, Benvenuto Cellini took the heiligenschein as a sign that he above all others was blessed because

he saw it shining only on the dew around the shadow of *his* head and not the shadows of the heads of his companions. Somehow, he never thought to ask his companions if they saw the heiligenschein around their blessed heads.



Fig. 9-61. Antisolar glow on dry grass, 29 Sept 2017. Jan Curtis.



Fig. 9-62. Heiligenschein cause by dew on the grass 05 Feb 2025. SDG.

9.8 Rainbow and Ray Gallery



Fig. 9-63. Hail streaks without raindrops blot out rainbows. Where there is only hail the bow will fail. Anticrepuscular rays cross the bow at right. Cheyenne, WY, 02 Aug 2020. Jan Curtis.



Fig. 9-64. Blue sky double rainbow from dying shower facing Catalina Mountains from Vail AZ, 22 Jun 2022. Jan Curtis.



Fig. 9-65. Blue shaded crepuscular rays in smoky air, 31 Jul 2025. Jan Curtis.



Fig. 9-66. Two color twilight sky – crepuscular ray due to shadow of thunderstorm 500 km away over the horizon. 10 Sep 2018. Jan Curtis.



Fig. 9-67. Double rainbow with supernumeraries at sunset, Cheyenne, WY, 26 Jul 2024. Jan Curtis.